Experimental comparison of N(1s) X-ray photoelectron spectroscopy binding energies of hard and elastic amorphous carbon nitride films with reference organic compounds

W.J. Gammon[a],*, O. Kraft[b], A.C. Reilly[a], B.C. Holloway[c]

[a]*Department of Physics, College of William and Mary, Williamsburg, VA 23187, USA*
[b]*Max-Planck-Institut fur Metallforschung, Stuttgart, Germany*
[c]*Department of Applied Science, College of William and Mary, Williamsburg, VA 23187, USA*

Abstract

In this work, hard and elastic amorphous carbon nitride (a-CN_x) films were deposited by DC magnetron sputtering on heated Si(001) substrates at 400 °C. Nanoindentation results confirmed that the films were highly compliant and had high elastic recovery. X-ray photoelectron spectroscopy (XPS) was used to investigate nitrogen bonding by directly comparing the N(1s) spectra of a-CN_x with the N(1s) peak positions of a variety of organic compounds that were characterized in the same XPS system. The N(1s) XPS spectra of hard and elastic a-CN_x is resolved into two dominant intensity contributions at 398.5 and 400.6 eV. We show that the N(1s) spectra of a-CN_x do not conclusively support a film-structure model with nitrogens bonded to sp^3 carbons. We offer an alternate interpretation based on the presented data and previous XPS, nuclear magnetic resonance (NMR), and computational work. Together, the data suggest that hard and elastic a-CN_x consists of an sp^2 carbon network and that single-atom vacancy defects, as found in a graphite layer, may be present in the material. This implies that the low binding energy N(1s) component at 398.5 eV may be due to pyridine-like nitrogen bonded at the perimeter of a vacancy defect.
© 2003 Elsevier Ltd. All rights reserved.

Keywords: A. Carbon films; B. Plasma sputtering; C. X-ray photoelectron spectroscopy; D. Chemical structure, Mechanical properties

1. Introduction

Researchers have found that incorporating nitrogen into carbon films dramatically alters their mechanical properties. Under favorable deposition conditions, amorphous carbon nitride (a-CN_x) films can be fabricated with high recovery [1,2]. The material gives when pressed on and recovers its original shape when the load is released, as it has a rather low modulus but high strength. Therefore, it can be regarded as an elastic and hard material. Ordinarily, hard materials such as ceramics have high modulus and are brittle, while soft materials such as metals have a low modulus and deform plastically. Thus, the mechanical properties of a-CN_x films are unusual. However, it is

important to realize that a-CN_x is a relatively new material. In order to make technological applications more feasible for this material, the most fundamental question needs to be answered: How does the addition of nitrogen in carbon films affect the bonding and improve mechanical properties? A basic understanding of nitrogen bonding is needed before other important technical issues such as degradation and adherence of a-CN_x thin films can be justly considered.

In previous studies, X-ray photoelectron spectroscopy (XPS) has been used to examine the composition of a-CN_x films. Several groups have measured high-resolution XPS spectra of the N(1s) core levels; however, fits to deconvolute the spectra and peak assignments vary in the literature [1–5]. The experimental N(1s) spectra of hard and elastic a-CN_x are typically resolved into three intensity contributions by fitting Gaussian line-shapes. The two major components to the intensity are typically near 400.6 and

---

*Corresponding author. Tel.: +1-757-221-1893; fax: +1-757-221-3540.

E-mail address: jgammon@physics.wm.edu (W.J. Gammon).

398.5 eV. The absolute position and relative intensity of these peaks seem to be dependent on deposition temperature and are correlated with the mechanical properties of the film [1,2,4]. The remaining component is described by a broad, high-binding-energy shoulder near 402 eV [1]. However, the actual bonding configurations responsible for the chemically shifted peaks are not understood.

In this work, we have measured XPS spectra of several organic compounds representative of various nitrogen bonding configurations in carbon and nitrogen materials. These reference spectra were compared with XPS data from hard and elastic a-CN$_x$ thin films. We show that the assignment of the low binding energy N(1s) component as due to nitrogen bonded to sp^3 carbons is not conclusive. We suggest that this component is instead due to pyridine-like nitrogen bonded at the perimeter of a vacancy defect. This defect may be similar to a single-atom vacancy in a graphite layer.

2. Experimental

Thin film deposition of a-CN$_x$ on Si(001) was accomplished by DC magnetron sputtering in a pure nitrogen discharge at 0.7 Pa using a US Inc. 50-mm Mightymak sputtering gun. The target was a 50 mm-diam. and 6.4 mm-thick, 99.999% pure graphite disk. The sample was mounted on a radiatively heated substrate holder, 5 cm from the target. The a-CN$_x$ films were deposited at 400 °C. The ultimate pressure of the vacuum system was 4×10^{-5} Pa at room temperature.

Prior to putting the 1 cm^2 silicon substrates in the vacuum system, they were ultrasonically cleaned in an acetone bath followed by a bath in isopropanol, for 10 min each. Before deposition, the target was sputter cleaned for 10 min with a shutter in position to block the substrate, and the substrates were heated in-situ at 850 °C for 10 min. The film deposition rate was determined to be ~1 μm/h at 400 °C as determined by a thickness profile measurement with scanning electron microscopy. Deposition times were typically 1–2 h and never less than 1 h. For all depositions, the target was current limited at 300 mA at a discharge voltage of approximately −660 V, with the substrate bias held at ground. Mechanical testing on the a-CN$_x$ films was carried out with a MTS NanoXP nanoindentation system using a Berkovich tip. The indentations were performed to a depth of about 100 nm under a constant strain rate condition by keeping $\dot{P}/P$ constant, where $\dot{P}$ and P denote the load rate and load, respectively.

The organic compounds for this study (see Table 1) were purchased from Aldrich in powder form with a purity of no less than 97%. The choice of reference compounds was restricted by the following two constraints: (1) N atoms are bonded only to C or N up to second nearest neighbor; and (2) only one N bonding configuration per compound. In addition, none of the reference compounds

has an sp^3 bonded carbon component; although we do compare with computational results that consider sp^3 carbons. The powders were pressed into indium foil and excess material was blown off with compressed air. The entire indium surface was completely covered to ensure that no bare metal surface was exposed. This precaution was taken to eliminate differential charging of the substrate surface during XPS analysis.

XPS measurements were all performed ex-situ. XPS on the a-CN$_x$ films and on the organic compounds were carried out in a VG ESCA lab system with hemispherical energy analyzer and a non-monochromated Mg-Kα source. The spectrometer was calibrated using the Au 4f$_{7/2}$ peak at 84.0 eV with a full-width half-maximum (FWHM) of 1.5 eV at 50 eV pass energy. No presputter step was carried out prior to acquiring the spectra. Base pressure during analysis was typically 1×10^{-7} Pa for the a-CN$_x$ thin films. However, due to high vapor pressures of the organic powders, spectra were acquired at pressures as high as 1×10^{-5} Pa with exception to acridine. The spectra of acridine were acquired at $\sim 2 \times 10^{-4}$ Pa due to its high vapor pressure.

To compensate for sample charging, all binding energies were referenced to the low binding energy component of the C(1s) spectrum, which was assigned a value of 284.6 eV. The reference binding energy was chosen to match the C(1s) binding energy of graphite powder at 284.6 eV, as measured by our XPS system. The position of the low binding energy component was determined by a least-squares fit of Gaussian components to the spectrum. For the organic compounds listed in Table 1, charge compensation was accomplished by fitting the C(1s) spectrum with one or two Gaussian components, depending on the asymmetry of the spectrum. The low binding energy C(1s) component was then charge shifted to 284.6 eV. For the a-CN$_x$ thin films, the C(1s) spectrum always required a fit with more than one Gaussian component, and in this case the position of the low binding energy component was determined by a least squares fit of four components to the C(1s) spectrum, with each constrained to have the same FWHM (usually 2.1 eV). The charge shift correction, as determined by this method, was typically 0.3 eV for the a-CN$_x$ films.

3. Results

Nanoindentation was used to confirm that the material deposited at 400 °C was in fact the high elastic recovery material previously studied [1,2,6–8]. Typical nanoindentation data of a-CN$_x$ deposited at 400 °C is shown in Fig. 1, which illustrates the behavior of the material under load. In particular, the material exhibits highly elastic behavior but resists plastic deformation. The unloading portion of the data was fit with the power–law relation as described by Oliver and Pharr [9], and this fit is shown in

Table 1
The chemical names, N(1s) binding energies, and the experimental vs. expected N/C ratios are shown for the structures **B**–**E** in Fig. 2
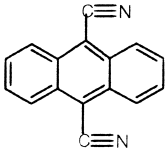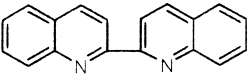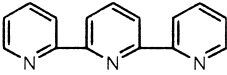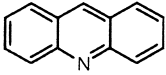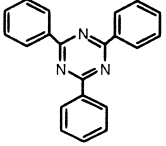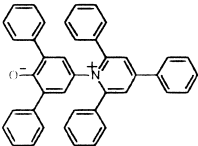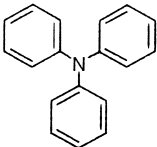
	Name	9,10-Anthracenedicarbonitrite
	N(1s) Binding Energy (eV)	399.0
	N/C measured	0.125
	N/C expected	0.125
	Name	2,2′-Biquinoline
	N(1s) Binding Energy (eV)	398.4
	N/C measured	0.086
	N/C expected	0.111
	Name	2,2′:6′2″-Terpyridine
	N(1s) Binding Energy (eV)	398.5
	N/C measured	0.169
	N/C expected	0.200
	Name	Acridine
	N(1s) Binding Energy (eV)	399.2
	N/C measured	0.078
	N/C expected	0.077
	Name	2,4,6-Triphenyl-1,3,5-Triazine
	N(1s) Binding Energy (eV)	398.9
	N/C measured	0.141
	N/C expected	0.143
	Name	Reichardt's Dye
	N(1s) Binding Energy (eV)	401.7
	N/C measured	0.020
	N/C expected	0.024
	Name	Triphenylamine
	N(1s) Binding Energy (eV)	399.9
	N/C measured	0.060
	N/C expected	0.056

Fig. 1. A power–law exponent of 2 was found to best describe the contact area of the indenter tip. This exponent is typical for the contact of a conical indenter with an elastic half-space, which is unusual since exponents between 1.2 and 1.6 are typically observed for most materials [10]. Using this exponent, the residual displacement was determined by the best least-squares fit. The recovery, as defined by Zheng et al. [6], was determined by averaging over six indents and is given by 90±2% for an indentation depth of 120 nm and a maximum load of 0.9 mN. The recovery and power-law exponent as determined for this material are consistent with our earlier work [2]. In addition, for an indentation depth of 120 nm, nanoindenta-

tion tests give a hardness of 5.5±0.6 GPa, and an elastic modulus of 38±2 GPa.

A summary of the N(1s) XPS results on the reference organic compounds is graphically depicted in Fig. 2. The upper portion of Fig. 2 displays the N(1s) binding energies of the various reference organic compounds. Structures **A** and **F** are from the binding energy calculations by Souto et al. [11]. Structures labeled **B**–**E** are from our experimental XPS measurements. The diamond-capped histograms indicate the N(1s) binding energy for the above structures: **(A)** N sp^3 coordinated in a ring structure to sp^3 carbon (calculated); **(B)** N bonded in a pyridine-like configuration; **(C)** N bonded in an sp configuration (nitrile); **(D)** N sp^3
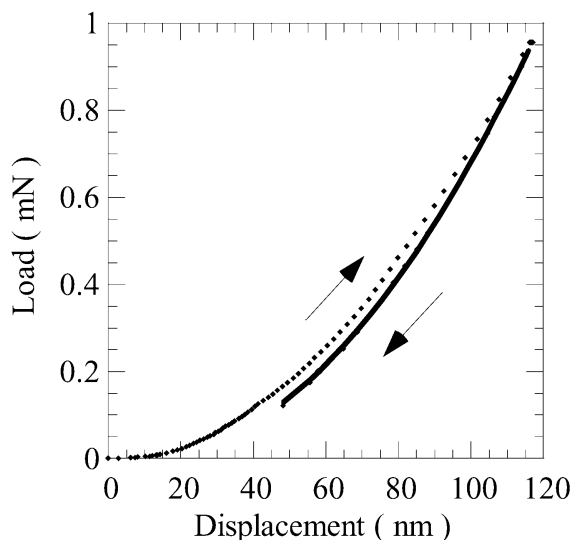
Fig. 1. Typical nanoindentation curve for an a-CN$_x$ film deposited at 400 °C. The unloading portion of the curve was fit with the power law relation as described by Oliver and Pharr [9].
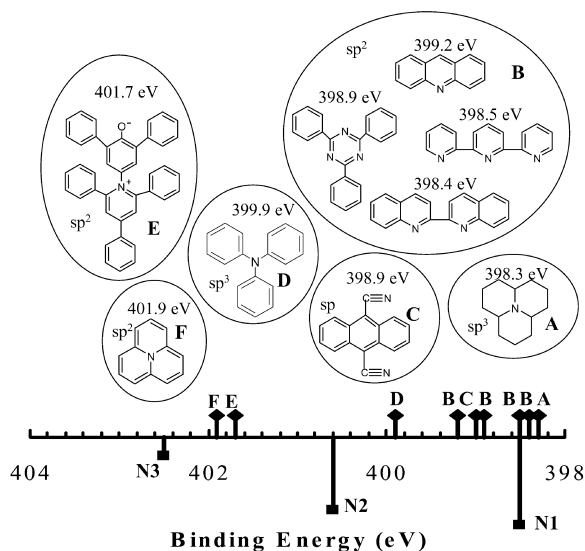

Fig. 2. Upper: N(1s) binding energies for a variety of carbon and nitrogen compounds. Structures **A** and **F** are from the binding energy calculations of Souto et al. [11]. Structures **B**–**E** are from our experimental XPS measurements. The histograms indicate the N(1s) binding energy for the above structures: (**A**) N sp^3 coordinated in a ring structure to sp^3 C; (**B**) N bonded in a pyridine-like configuration; (**C**) N bonded in a nitrile configuration (sp); (**D**) N sp^3 coordinated to aromatic rings; (**E**) N three-fold sp^2 bonded in a salt; and (**F**) N trigonally bonded in a graphite-like segment. Lower: The histograms (capped with filled squares) indicate the position of the N(1s) binding energy for the Gaussian components a-CN$_x$ (Fig. 3). The heights of the histograms indicate the relative fractional contribution of a particular Gaussian component.

coordinated to three aromatic rings; (**E**) N sp^2 bonded in a salt; and (**F**) N bonded to three sp^2 carbons in the interior of a graphite-like segment (calculated). The histograms labeled in the lower portion of Fig. 2 will be explained later. For convenience, Table 1 displays the chemical name, N(1s) binding energy, and the experimental vs. expected N/C ratios for the structures **B**–**E** (Fig. 2). The comparison of experimental vs. expected N/C ratios suggests that we are primarily measuring the C(1s) component of the compound and not measuring the C(1s) component of adventitious carbon. In addition, the FWHM of the N(1s) peaks for the reference organic compounds all fall in the range of 1.8–2.1 eV, except for acridine, which had a FWHM of 3.3 eV.

The N(1s) XPS spectrum of hard and elastic a-CN$_x$ is shown in Fig. 3. The material exhibits a typical at.% N concentration of 21% and exhibits a typical oxygen contamination of 5%, as determined by XPS. The observed O(1s) signal is attributed to exposure to atmosphere during sample transport for XPS analysis. Before fitting the data, an integral background was calculated by an iterative Shirley method [12] and subtracted from the raw data. Gaussian components were fit to the N(1s) spectra, as illustrated in Fig. 3, and these components were constrained to have the same FWHM. The N(1s) peak is composed of the components labeled N1, N2, N3, and N4 at 398.5, 400.6, 402.5, and 404.8 eV, respectively, and each has a FWHM of 2.2 eV. The relative fractions of N1, N2, N3, and N4 are 48, 39, 10 and 3%, respectively. The gray
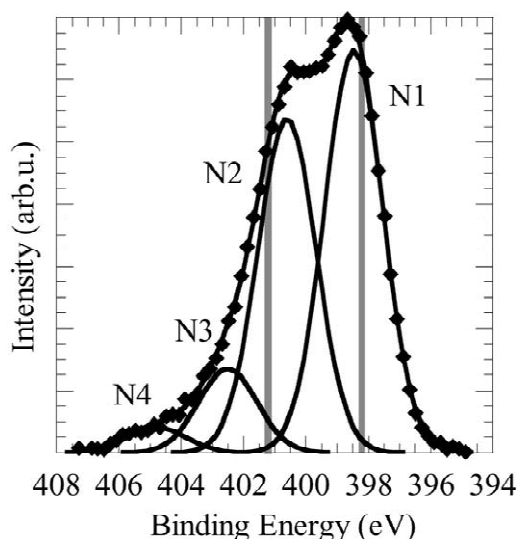
Fig. 3. A typical N(1s) XPS spectra of a-CN$_x$ deposited at 400 °C. The spectra were fit with Gaussian line-shapes after subtracting an integral background. The gray vertical lines indicate the experimental N(1s) binding energies of the two components of 3,5,11,13-tetraazacycl[3.3.3]azine as measured by Boutique et al. [13].
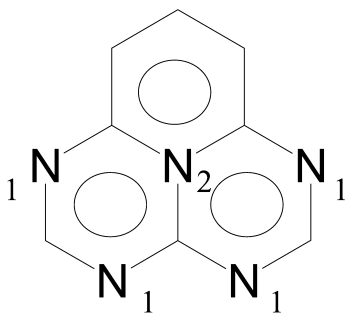
Fig. 4. A schematic of the structure of 3,5,11,13-tetra-azacycl[3.3.3]azine. The pyridine-like N bonding configurations (N1) exhibit an XPS binding energy of 398.3 eV, and the three-fold coordinated sp^2 N bonding configuration (N2) exhibits a binding energy of 401.3 eV [13].

vertical lines indicate the experimental N(1s) binding energies of the two components of 3,5,11,13-tetra-azacycl[3.3.3]azine as measured by Boutique et al. [13] and are shown for comparison purposes. The two components of 3,5,11,13-tetraazacycl[3.3.3]azine at 398.3 and 401.3 eV exhibit a 3.0 eV chemical shift, and the structure of this compound is shown in Fig. 4. The spectral features of the reference organic compounds (Fig. 2) were compared to the XPS spectra of a-CN$_x$ (Fig. 3) to indicate chemical bonding. In the lower portion of Fig. 2, the histograms (capped with filled squares) denote the N(1s) binding energies of the various Gaussian components N1, N2, and N3 (for simplicity N4 is not shown). The heights of the histograms indicate the relative fractional contribution of a particular Gaussian component. Interpretation of these various components is discussed below.

4. Discussion

Binding energy calculations by Johansson et al. [14] suggest the following interpretation of the two main N(1s) bonding contributions. They proposed that the N(1s) peaks at 398.5 and 400.6 eV in hard and elastic a-CN$_x$, were due to (1) sp^3 nitrogen bonded to sp^3 hybridized carbon; and to (2) sp^2 nitrogen substituted in the interior of a graphitic segment, respectively. This interpretation supports the phenomenological model that the hardness of a-CN$_x$ films is due to cross-linking of graphitic planes by sp^3 bonded carbons [14] and appears to be widely accepted in the literature.

The bonding model as proposed by Johansson et al. [14] suggests that the mechanical robustness of hard and elastic a-CN$_x$ is due to an increase of sp^3 bonded nitrogen in an sp^3 carbon environment, as in the model amine structure $N(C(CH_3)_3)_3$. However, these structures may be unstable in a-CN$_x$ as indicated by recent experimental evidence [15], which suggests an sp^3 coordinated carbon environ-

ment will relax to sp^2 in the presence of approximately 14% bonded nitrogen. In addition, recent ^{13}C nuclear magnetic resonance (NMR) results indicate that hard and elastic a-CN$_x$ consists of an aromatic carbon structure and that sp^3 bonded carbons are absent [8]. It thus can be inferred that the bonding model proposed by Johansson et al. [14] is incompatible with the film structure of a-CN$_x$.

Computational work by Snis and Matar [16,17] on core-level binding energies of various carbon nitride phases offers another interpretation of the ~2 eV chemical shift between the two main components in the N(1s) spectrum. Their calculations on the model carbon nitride compound, $C_{11}N_4$, distinguish two N(1s) binding energy ranges which are associated with the two nonequivalent nitrogen positions on the perimeter of a single-atom vacancy in a graphitic layer. The two nitrogen bonding configurations in $C_{11}N_4$ are (1) sp^2 N bonded to three sp^2 carbons (400.8–401.3 eV) and (2) sp^2 N bonded to two sp^2 carbons (398.3–398.8 eV) [17]. The chemical shift between these two components is consistent with the core-level shift of the two main components in the XPS spectra of hard and elastic a-CN$_x$ [1,2]. Snis and Matar's model can account for the experimentally observed chemical shift between N1 and N2 and is consistent with our recent NMR results, which indicate that hard and elastic a-CN$_x$ is composed of an sp^2 carbon network with less than 0.1% sp^3 bonded carbons [8].

Experimental XPS analysis of the N(1s) peak of a-CN$_x$ has not clarified previous computational results. Instead, previous work has produced varying interpretations of the chemical bonding [1–5]. Even in this study, as shown in Fig. 2, the N(1s) peak of a-CN$_x$ exhibits bonding over the whole range of configurations. However, inspection of N(1s) binding energies for the various compounds (**A**–**F**) suggests three primary nitrogen binding energy regions: (1) a high binding energy region due to sp^2 nitrogen bonded in a salt-like configuration as in (**E**) or nitrogen bonded to three sp^2 carbons in a graphitic segment as in (**F**); (2) a midrange binding energy region which would include compounds like structure **D**; and (3) a low binding energy region due to sp^3 N bonded to sp^3 C (**A**) or pyridine-like (**B**) or nitrile (**C**). Also, as indicated in Fig. 2, a particular bonding configuration may cover a binding energy range of ~1.0 eV, and thus the overlap of spectral intensities between the regions may be expected. For example, the binding energy range for the pyridine-like compounds (structures labeled **B**) is 0.8 eV. In this discussion, we ignore the very high binding energy feature N4, since its overall contribution is small and its origin is poorly understood. It is worth mentioning that the XPS work by Marton et al. [3] on a-CN$_x$ has attributed the intensity in the range of N3 as due to N–O bonds. Clearly this possibility is not resolvable from the other the features **E** and **F** shown in Fig. 2; therefore, we can not dismiss this possibility. Although we do not consider N–O bonding any further in this paper, it is interesting to note that

structure **E** illustrates how charge transfer due to distant oxygen bonding can shift the N(1s) component to higher binding energy.

A discussion of N1 is very limited if only the comparison in Fig. 2 is considered, since its spectral intensity overlaps with the regions encompassed by the structures **A**–**C**. However, previous Fourier transform infrared spectroscopy studies have shown that the fraction of nitrile bonding is small in our hard and elastic a-CN$_x$ films [2]; therefore, we do not consider this arrangement any further. Disregarding nitrile bonding, Fig. 2 suggests that the spectral intensity of N1 is due to N bonded in a pyridine-like configuration (**B**), N trigonally bonded to sp^3 carbon (**A**), or a mixture of the two configurations. However, further experimental evidence by our recent ^{13}C NMR study on hard and elastic a-CN$_x$ indicates the absence of sp^3 bonded carbons [8]. Therefore, it is plausible to attribute N1 to a pyridine-like bonding configuration (**B**).

Discussion of the binding energy components N2 and N3 are complicated by the fact that neither one coincides with one of the three bonding regions depicted in Fig. 2. The binding energy of N2 at 400.6 eV falls in a range between pyridine-like compounds (**B**) and nitrogen threefold coordinated to sp^2 carbons (**E** and **F**). While, the binding energy of N3 at 402.5 eV is ~1 eV higher than the structures **E** and **F**.

Interestingly, the N(1s) binding energy of triphenylamine (**D**) at 399.9 eV falls the closest to the binding energy of N2. However, it is not clear from the limited experimental data that N2 can be attributed to this configuration. Although, it is interesting to point out that the binding energy of triphenylamine is consistent with other values reported for amines [18]. In addition, XPS analysis of coals and chars by Pels et al. [18] offer another interpretation, which suggests that the N(1s) component near 400.6 eV may be due to N bonded in a pentagon, as in a pyrrole-like configuration. Interestingly, the existence of pentagons has been suggested by Sjostrom et al. [7] to account for the buckled graphitic planes observed in a-CN$_x$. Another interpretation of N2 is offered by the computational work by Snis and Matar [16,17] on the model compound C$_{11}$N$_4$, which suggests N2 may be due to sp^2 N bonded to three sp^2 carbon neighbors in hexagons. At first glance, this assignment seems questionable, since structures **E** and **F** suggest that this bonding configuration should appear at higher binding energy. Moreover, measurements on 3,5,11,13-tetraazacycl[3.3.3]azine suggest a value closer to 401.3 eV (Fig. 4). However, computational work by Casanovas et al. [19] indicates that the binding energies associated with sp^2 N bonded to three sp^2 carbons in graphene segments fall in a broad range of 400.5–402.7 eV. In light of the available evidence, it seems likely that N2 could be ascribed to amine, pyrrole-like, nitrogen substituted in a graphene segment, or a mixture among these configurations. We must emphasize precise bonding assignment is not possible without further experimental data.

The peak component N3 at 402.5 eV in a-CN$_x$ may be due to threefold coordinated sp^2 N bonded to aromatic carbon. There are several possible bonding situations that would fall in this category: (1) N bonded at an interior site of a graphene segment (similar to structures in Fig. 4 and **F** in Fig. 2); (2) N bonded on the edge of a graphene segment; and (3) N bonded in a configuration similar to that of structure **E**. Even though the binding energy of **E** is 0.8 eV less than N3, we have included the possibility since a range of binding energies may be anticipated for similar bonding situations. These possible bonding assignments for N3 are consistent with the computational work by Casanovas et al. [19], which indicates nitrogens bonded in graphene segments have binding energies in the range of 400.5–402.7 eV.

In summary, it is plausible that N1 exhibits a pyridine-like bonding configuration. The computational work by Snis and Matar suggests that the N1 may be twofold coordinated nitrogen at the perimeter of vacancy defect structure as found in C$_{11}$N$_4$ [16,17]. In fact, the two nonequivalent nitrogen positions on the perimeter of a vacancy defect in C$_{11}$N$_4$ exhibit a chemical shift in the range of 2.0–3.1 eV. This is consistent with the chemical shift of 2.1 eV exhibited between the high binding energy type at 400.6 eV and the low binding energy type at 398.5 eV, as observed in our spectra (Fig. 3). The defect structure in C$_{11}$N$_4$ is formed around an empty site in a graphitic plane [16,17], and the empty site defect may give additional flexibility for bending, allowing the adjacent graphitic planes to intersect and cross-link together. In addition, a vacancy defect in a graphitic structure would provide space for the pyridine-like nitrogens to place their lone pairs. The driving force that would encourage plane buckling by these types of defects is not clear and is the subject of ongoing work. Although, it is worth mentioning that a pyrrole-like bonding configuration as suggested by the work of Pels et al. [18] and Sjostrom et al. [7] may provide a buckling mechanism (pentagon incorporation into a graphene sheet) that is consistent with XPS data.

5. Conclusions

In this work, amorphous carbon nitride (a-CN$_x$) films were deposited on heated Si(001) substrates by DC magnetron sputtering. Nanoindentation confirmed that our films are hard and highly elastic with very high elastic recovery. X-ray photoelectron spectroscopy (XPS) was used to investigate nitrogen bonding in a-CN$_x$ by directly comparing the carbon nitride N(1s) spectra with the peak positions from a variety of organic compounds.

Our XPS data support the assignment that the low binding energy N(1s) component, N1, at 398.5 eV is due to nitrogen bonded in a pyridine-like configuration, which stands in contrast with earlier peak assignments [1,7,14]. Assigning the low binding energy N(1s) component to sp^2 hybridization suggests that the nitrogen may be twofold

bonded at the perimeter of vacancy defect structure as found in $C_{11}N_4$ [16,17]. In fact, the two nitrogen bonding situations in $C_{11}N_4$ along the perimeter of the defect exhibit a chemical shift that is consistent with the our experimental spectra. The defect structure in $C_{11}N_4$ is formed around an empty graphitic site [16,17], and the empty site defect may give necessary flexibility for bending, allowing the adjacent graphitic planes to intersect and cross-link together. However, the driving force that would encourage plane buckling with these types of defects is not clear and is the subject of future work.

Acknowledgements

References

[1] Hellgren N, Johansson MP, Broitman E, Hultman L, Sundgren JE. Phys Rev B 1999;59:5162.

[2] Holloway BC, Kraft O, Shuh DK, Nix WD, Kelly M, Pianetta P, Hagstrom S. J Vac Sci Technol A 2000;18:2964.

[3] Marton D, Boyd KJ, Al-Bayati AH, Todorov SS, Rabalais JW. Phys Rev Lett 1994;73:118.

[4] Ronning C, Feldermann H, Merk R, Hofsass H, Reinke P, Thiele JU. Phys Rev B 1998;58:2207.

[5] Spaeth C, Kuhn M, Richter F, Falke U, Hietschold M, Kilper R, Kreissig U. Diamond Related Mater 1998;7:1727.

[6] Zheng WT, Sjostrom H, Ivanov I, Xing KZ, Broitman E, Salaneck WR, Greene JE, Sundgren JE. J Vac Sci Technol A 1996;14:2696.

[7] Sjostrom H, Stafstrom S, Boman M, Sundgren J-E. Phys Rev Lett 1995;75:1336.

[8] Gammon WJ, Malyarenko DI, Kraft O, Hoatson GL, Reilly AC, Holloway BC. Phys Rev B 2002;66:153402.

[9] Oliver WC, Pharr GM. J Mater Res 1992;7:1564.

[10] Brotzen FR. Int Mater Rev 1994;39:24.

[11] Souto S, Pickholz M, Dos Santos MC, Alvarez F. Phys Rev B 1998;57:2536.

[12] Proctor A, Sherwood MA. Anal Chem 1982;54:13.

[13] Boutique JP, Verbist JJ, Fripiat JG, Delhalle J, Pfister-Guillouzo G, Ashwell GJ. J Am Chem Soc 1984;106:4374.

[14] Johansson A, Stafstrom S. J Chem Phys 1999;111:3203.

[15] Jiangtao H, Peidong Y, Lieber CM. Phys Rev B 1998;57:R3185.

[16] Snis A, Matar SF, Plashkevych O, Agren H. J Chem Phys 1999;111:9678.

[17] Snis A, Matar SF. Phys Rev B 1999;60:10855.

[18] Pels JR, Kapteijn F, Moulijn JA, Zhu Q, Thomas KM. Carbon 1995;33:1641.

[19] Casanovas J, Ricart JM, Rubio J, Illas F, Jimenez-Mateos JM. J Am Chem Soc 1996;118:8071.